



PII S0016-7037(00)00487-7

The dissolution kinetics of amorphous silica into sodium chloride solutions: Effects of temperature and ionic strength

JONATHAN P. ICENHOWER[†] and PATRICIA M. DOVE*

School of Earth and Atmospheric Sciences, Georgia Institute of Technology, Atlanta, GA 30332-0340, USA

(Received August 23, 1999; accepted in revised form June 29, 2000)

Abstract—The kinetics of amorphous silica, SiO₂ (am), dissolution was quantified in deionized water and NaCl solutions. By using two sources of pure SiO₂ glass (fused purified quartz and pyrolyzed SiCl₄), rates were measured at 40°C to 250°C by applying three types of reactor systems to assess kinetic behavior over the full temperature range. Dissolution rates of the two materials are similar within experimental error. Absolute rates of amorphous silica dissolution in deionized water exhibit an experimental activation energy, $E_{a,sp}$, of 81.9 ± 3.0 and 76.4 ± 6.6 kJ/mol for the fused quartz and pyrolyzed silica, respectively. These values are similar to estimates for quartz within experimental errors. Absolute dissolution rates of SiO₂ (am) in deionized water are $\sim 10\times$ faster compared to quartz. Amorphous silica dissolution rates are significantly enhanced with the introduction of NaCl to near-neutral pH solutions such that 0.05 molal sodium ion enhances rates by $21\times$ compared to deionized water. The new kinetic data are combined with previous measurements of SiO₂(am) dissolution rates in ‘pure’ water to evaluate the temperature dependence of dissolution. The comprehensive data set spans 25°C to 250°C and yields the Arrhenius expression $\log k_+ = 0.82191 - 3892.3/T(K)$ to give an apparent activation energy for dissolution of 74.5 ± 1.4 kJ/mol. These findings step toward the larger goal of understanding silica polymorph reactivity in the complex fluid compositions of natural systems. Copyright © 2000 Elsevier Science Ltd

1. INTRODUCTION

Silica polymorphs are prevalent within diverse marine and terrestrial environments and comprise a significant fraction of the Earth’s crust. Of the nine recognized polymorphs, the crystalline varieties of SiO₂ have received the greatest scrutiny to date. Numerous experimental studies have investigated the dissolution kinetics of α -quartz (e.g., Knauss and Wolery, 1988; Bennett et al., 1988; Brady and Walther, 1990; Dove and Crerar, 1990; House and Orr, 1992; Tester et al., 1994) and a coherent, although incomplete, picture has emerged regarding the mechanisms of dissolution.

In contrast, relatively little is understood regarding the dissolution kinetics of amorphous forms of silica. In natural environments, amorphous silica, SiO₂(am), has widespread occurrence as a result of numerous inorganic and biologically mediated processes. Combined with the recognition that this solid-phase silica reservoir is more reactive than its crystalline counterparts, a knowledge of the fundamental controls on the dissolution mechanisms of SiO₂(am) is prerequisite to accurate models of silica movement between mineral and aqueous reservoirs within the silicon biogeochemical cycle.

Rationale for understanding the reactivity of silica polymorphs are also found on a broader scale in the context of understanding the physical and chemical phenomena that govern the reactivity of simple Si-O bonded phases. These minerals and materials constitute the end-member composition of highly complex silica phases. Because the SiO₄ moiety is the funda-

mental structural component of silicate minerals and glasses found in nature, the chemical durability of the Si-O bond has a strong bearing on the overall dissolution behavior of earth materials. It is recognized that the extent to which SiO₄ tetrahedra are cross-linked in a mineral or glass impacts the dissolution rates and leaching behavior of silicate minerals and glasses (e.g., review in Casey and Bunker, 1990). For example, Grambow (1985) found that the rate-limiting step in the overall breakdown of the glass is governed by dissolution of the SiO₄ network. Thus, the corrosion resistance of the SiO₄ network is reflected in the aggregate reactivity of both crystalline and amorphous materials. This theme is echoed in studies of the complex engineered glass compositions that are proposed worldwide to host nuclear wastes.

A central issue in amorphous or glassy systems is the magnitude of SiO₄ reactivity in a framework that lacks long-range order. Students of the Earth intuitively recognize that the amorphous forms of silica dissolve more quickly than their crystalline counterparts, and there is evidence to corroborate this, as detailed below. The contrast in dissolution behavior can be attributed to structural differences between SiO₂(am) and crystalline silica, but the physical nature of this variance remains elusive. Therefore, dependence of SiO₂(am) dissolution rates on solution chemistry and temperature cannot be inferred with full confidence from the more comprehensive quartz dissolution studies.

1.1. Previous Investigations and Rationale for this Study

Studies that quantify the kinetics of amorphous silica dissolution are few and the findings, although important, show significant gaps in our quantitative understanding of SiO₂(am) reactivity. First, previous experimental investigations of SiO₂(am) reactivity report few data as summarized in Table 1

* Corresponding author and new address: Dept. Geological Sciences, Virginia Polytechnic Inst. and State Univ., Blacksburg, VA 24061 USA (dove@vt.edu).

[†] Present address: Pacific Northwest National Laboratory, Applied Geology and Geochemistry Group, Richland, WA 99352.

Table 1. Summary of amorphous silica dissolution rate measurements conducted in deionized or distilled water. These measurements are plotted in Figure 4.

Reference	Temp °C	Log Rate mol/m ² /s
Elmer and Nordberg (1958)	95°	-11.6
Rimstidt and Barnes (1980)	18°	-9.95
Mazer and Walther (1994)	40°	-11.5
	60°	-10.4
	85°	-9.5
Seidel et al. (1997)	25°	-12.0

for rates measured in 'pure' water (distilled or deionized). The experimental investigation of Rimstidt and Barnes (1980) stands as a classic study of silica kinetics, but these investigators reported only one rate measurement of SiO₂(am) dissolution (e.g., Table 1). Possible rate-enhancing effects of Na⁺ and other alkali and alkaline earth cations on the dissolution of silica polymorphs were not recognized at the time. At first glance, this conclusion appears to be reinforced by experimental evidence from Wirth and Gieskes (1979). They determined that varying the ionic strength of solutions caused only small changes in SiO₂(am) dissolution rates. However, they were interested in systems with high salinities, which, as shown later, are at concentrations where rates become less sensitive to differences in ionic strength.

The problem of a relatively sparse data set has continued the debate over the temperature dependence of amorphous silica dissolution. Mazer and Walther (1994) reported rate data for the dissolution of SiO₂(am) and determined an activation energy of 93 ± 15 kJ/mol from three experiments conducted over the relatively narrow temperature range of 40°C to 85°C. This value is significantly larger than the ~60 to 65 kJ/mol values estimated by Rimstidt and Barnes (1980) and adds further uncertainty to appraisals of dissolution rates and to extrapolations of reaction rates to higher temperatures.

The purpose of this paper is to establish relationships between temperature and the ionic strength of solution and the dissolution kinetics of SiO₂(am). Accordingly, one goal of this study is to determine dissolution rates over a larger temperature interval. This objective requires that we use three different experimental apparatuses, so we also assess the agreement between rate data obtained by the various techniques. By combining rates from the previous investigations with the new data presented in this study, we evaluate the temperature dependence of dissolution as one comprehensive data set. A further aim of this study is to consider the effects of dissolved solutes on SiO₂(am) reactivity. Because sodium is the most abundant cation in natural waters, we investigate the rate-enhancing effect of NaCl solutions on the dissolution kinetics of amorphous silica. Comparisons with published quartz dissolution rate measurements for similar solution compositions provide an opportunity to examine the control of structure on the rate-enhancing ability of this important ion while holding the mineral/material composition invariant.

Table 2. Chemical compositions of amorphous silica materials used in this study as determined by ICP-AES.

Wt.% oxide	Corning (treated)	QSI (treated)	QSI (untreated)
SiO ₂	99.97	100.15	100.11
Al ₂ O ₃	0	0.03	0.03
Fe ₂ O ₃	0.24	0.2	0.33
MnO	0	0	0
MgO	0	0	0
CaO	0	0	0
Na ₂ O	0	0	0
K ₂ O	0	0	0
TiO ₂	0	0	0
P ₂ O ₅	0	0	0
LOI ^a	0.12	0.1	0.09
Total	100.33	100.48	100.56
<i>Trace elements, ppm^b</i>			
Al	0	159	159
Fe	1679	1399	2308
Mn	0	0	0
Mg	0	0	0
Ca	0	0	0
Na	0	0	0
K	0	0	0
Ti	0	0	0
P	0	0	0
Ba	0	0	2
Zr	6	6	8
Sr	0	0	0
Y	0	0	0
Sc	0	0	0
Be	0	0	0
V	0	0	0

^a LOL = loss on ignition.

^b 0 = below detection limit.

2. METHODS

2.1. Sources and Characteristics of Amorphous Silica Run Materials

Amorphous silica materials used in these experiments were obtained from Quartz Scientific (Sunnyvale, CA, USA; QSI) and Corning (Corning, NY, USA). The QSI SiO₂(am) is manufactured by fusion of mechanically and chemically purified quartz whereas the Corning SiO₂(am) is produced by flame pyrolysis of SiCl₄ gas in the presence of oxygen. Both samples of amorphous silica reportedly contain low concentrations of impurities (including Al, B, alkali, and alkaline earth ions) on the order of ≤5 ppm each. Analyses of the samples by ICP-AES (Table 2) indicate that the concentrations of impurities are indeed low. Untreated and treated (defined below) QSI silica contain ~2,300 and ~1,300 ppm Fe, respectively; the Corning glass contains ~1,680 ppm Fe. In addition, the QSI glass may contain small concentrations of Al (up to ~160 ppm), but this value is near the Al detection threshold. The QSI glass reportedly does not contain water, but the Corning SiO₂(am) contains ~1,000 ppm OH (Jim Dickinson, pers. comm., 1998). Small quantities of water may be dissolved into silica during production by the reaction:



where Si-O-Si indicates a bridging oxygen between two Si atoms (e.g., Brückner, 1970). This reaction represents the breakdown of fully polymerized species to produce a glass structure with less polymerized species. Small quantities of dissolved OH have profound effects on silica glass properties. For, addition of only 1,200 ppm OH to dry SiO₂(am) lowers the measured glass transition temperature ~220 K (Brückner, 1970; Richet and Bottinga, 1984). We might expect, therefore, that the two types of glass would manifest differences in disso-

Table 3. Experimental conditions and measured dissolution rates of SiO₂(am) by using the hydrothermal mixed flow reactors (HMFR). All experiments were conducted at pH_{25°C} ~ 5.7.

Sample	Temp (°C)	NaCl conc. (molal)	Log average			Notes
			Flow rate (kg/s)	Silica (molal)	Log rate (mol/m ² s)	
Corning glass						
*19-19	250	0	-4.10	-3.79	-6.59	4
*19-1	225	0	-4.02	-4.15	-6.86	4
*20-1	225	0	-4.10	-4.16	-6.96	4
*19-4	200	0	-4.02	-4.68	-7.40	4
*20-4	200	0	-4.04	-4.60	-7.34	4
*19-7	175	0	-4.02	-5.17	-7.89	4
*20-7	175	0	-4.02	-5.01	-7.74	4
*19-22	150	0	-4.58	-5.14	-8.41	4
*20-22	150	0	-4.52	-5.31	-8.53	4
*1-25	200	0.01	-4.17	-3.43	-6.37	2
*3-13	200	0.01	-4.40	-3.16	-6.34	2
*4-13	200	0.01	-4.44	-3.38	-6.59	2
*5-37	200	0.01	-4.40	-3.33	-6.53	2
*6-37	200	0.01	-4.43	-3.13	-6.36	2
*1-34	180	0.01	-4.44	-3.54	-6.75	2
*3-28	180	0.01	-4.11	-3.88	-6.76	2
*4-28	180	0.01	-4.09	-3.86	-6.72	2
*3-41	160	0.01	-4.10	-4.27	-7.14	2
*4-41	160	0.01	-4.08	-4.26	-7.11	2
*4-50	140	0.01	-4.32	-4.52	-7.61	2
*5-40	140	0.01	-4.40	-4.52	-7.73	2
*6-40	140	0.01	-4.42	-4.42	-7.65	2
*5-46	120	0.01	-4.34	-5.09	-8.24	2
*6-46	120	0.01	-4.33	-5.11	-8.25	2
*1-28	200	0.03	-4.30	-3.01	-6.09	2
*3-16	200	0.03	-4.40	-2.92	-6.09	2
*1-22	200	0.05	-4.16	-3.07	-6.00	2
*3-4	200	0.05	-4.33	-2.94	-6.04	2
*4-4	200	0.05	-4.35	-3.00	-6.11	2
*3-7	200	0.05	-4.33	-2.85	-5.95	2
*4-7	200	0.05	-4.34	-2.99	-6.10	2
*3-10	200	0.05	-4.33	-2.87	-5.96	2
*4-10	200	0.05	-4.35	-3.02	-6.14	2
*5-31	200	0.05	-3.97	-3.17	-5.95	2
*6-31	200	0.05	-3.99	-3.11	-5.91	2
*5-34	200	0.05	-4.50	-2.92	-6.23	2
*6-34	200	0.05	-4.49	-2.76	-6.05	2
*19-37	200	0.05	-4.06	-3.17	-5.93	4
*20-37	200	0.05	-4.09	-3.21	-6.00	4
*1-31	180	0.05	-4.29	-3.28	-6.34	2
*3-25	180	0.05	-4.23	-3.38	-6.37	2
*4-25	180	0.05	-4.23	-3.43	-6.43	2
*19-34	175	0.05	-4.03	-3.77	-6.50	4
*20-34	175	0.05	-4.05	-3.92	-6.67	4
*3-44	160	0.05	-4.10	-3.91	-6.78	2
*4-44	160	0.05	-4.08	-3.86	-6.71	2
*19-25	150	0.05	-4.72	-3.58	-6.99	4
*20-25	150	0.05	-4.71	-3.31	-6.72	4
*4-53	140	0.03	-3.88	-4.63	-7.28	2
*4-47	140	0.05	-3.90	-4.55	-7.22	2
*5-43	140	0.05	-3.92	-4.57	-7.29	2
*6-43	140	0.05	-3.91	-4.65	-7.37	2
*4-56	120	0.05	-4.53	-4.52	-7.82	2
*5-49	120	0.05	-4.19	-4.80	-7.80	2
*6-49	120	0.05	-4.18	-4.90	-7.88	2
*5-52	100	0.05	-4.66	-5.00	-8.46	2
*6-52	100	0.05	-4.68	-5.06	-8.54	2
*19-28	100	0.05	-4.73	-5.22	-8.65	4
*20-28	100	0.05	-4.73	-5.24	-8.66	4
*3-19	200	0.07	-4.31	-2.83	-5.91	2
*4-19	200	0.07	-4.29	-2.96	-6.02	2
*5-28	200	0.1	-3.97	-2.98	-5.76	2

(Continued)

Table 3. (Continued)

Sample	Temp (°C)	NaCl conc. (molal)	Log average			Notes
			Flow rate (kg/s)	Silica (molal)	Log rate (mol/m ² s)	
*6-28	200	0.1	-3.95	-2.88	-5.64	2
*3-22	200	0.15	-4.30	-2.75	-5.82	2
*4-22	200	0.15	-4.29	-2.83	-5.89	2
*17-16	225	0	-4.15	-3.89	-6.86	5
*18-16	225	0	-4.18	-4.06	-7.05	5
*17-1	200	0	-4.45	-3.97	-7.24	5
*18-1	200	0	-4.45	-4.00	-7.27	5
*17-4	175	0	-4.44	-4.71	-7.97	5
*18-4	175	0	-4.44	-4.84	-8.10	5
*18-7	150	0	-4.46	-4.97	-8.24	5
*17-13	125	0	-4.87	-5.05	-8.75	5
*17-10	100	0	-4.79	-5.74	-9.36	5, 6
*18-10	100	0	-4.79	-5.94	-9.54	5, 6
*11-28	200	0.005	-4.01	-3.77	-6.80	3
*12-28	200	0.005	-4.02	-3.73	-6.78	3
*11-31	200	0.01	-4.17	-3.53	-6.73	3
*12-31	200	0.01	-4.18	-3.42	-6.63	3
*11-52	200	0.03	-3.91	-3.42	-6.35	3
*12-52	200	0.03	-3.88	-3.44	-6.33	3
*11-34	200	0.05	-4.02	-3.24	-6.27	3
*12-34	200	0.05	-4.02	-3.17	-6.22	3
*17-28	200	0.05	-4.11	-2.98	-5.91	5
*18-28	200	0.05	-4.05	-3.06	-5.93	5
*17-46	175	0.05	-4.02	-3.51	-6.34	5
*18-46	175	0.05	-4.00	-3.58	-6.39	5
*11-37	150	0.05	-4.51	-3.80	-7.33	3
*12-37	150	0.05	-4.52	-3.67	-7.22	3
*17-40	150	0.05	-4.49	-3.72	-7.03	5
*18-40	150	0.05	-4.48	-3.73	-7.03	5
*11-49	125	0.05	-4.53	-4.42	-7.97	3
*12-49	125	0.05	-4.39	-4.39	-7.80	3
*17-37	125	0.05	-4.59	-4.36	-7.77	5
*18-37	125	0.05	-4.56	-4.36	-7.73	5
*11-40	100	0.05	-4.50	-5.19	-8.72	3
*12-40	100	0.05	-4.52	-5.02	-8.56	3
*17-34	100	0.05	-4.75	-4.47	-8.04	5
*18-34	100	0.05	-4.72	-4.80	-8.33	5
*11-43	80	0.05	-4.67	-5.66	-9.35	3
*12-43	80	0.05	-4.65	-5.67	-9.34	3
*11-55	200	0.15	-3.89	-2.99	-5.90	3
*12-55	200	0.15	-3.88	-2.98	-5.88	3

Notes: 1) Surface area = 0.0248 m²/g; 2) Surface area = 0.0294 m²/g; 3) Surface area = 0.0261 m²/g; 4) Surface area = 0.025 m²/g; 5) Surface area = 0.033 m²/g; 6) Data not plotted or used to evaluate Ea.

lution rates given the potentially significant concentration of water in the Corning sample (see Section 3.1).

2.2. Preparation of Amorphous Silica Run Materials

The QSI and Corning SiO₂(am) materials were prepared by washing in separate methanol baths followed by H₂O₂ (30% vol.) baths. The samples were then immersed for 3 days in a 10% (vol.) nitric acid solution to remove any surficial impurities. The two materials were then ground in a ball mill and sieved to obtain the 300–425 μm or 200–300 μm fractions. These crushed samples subsequently underwent a second round of cleaning by 10% nitric acid (3 days) to remove any impurities imparted during the milling procedure (“treated” sample; see Table 2). This material was rinsed in deionized water and the solutions were decanted at least 12 times to remove fine-grained particles that may have adhered to the desired size fraction. We then immersed the samples in deionized water at 100°C for 12 to 24 h to dissolve remaining high-energy surface sites. Inspection of the starting

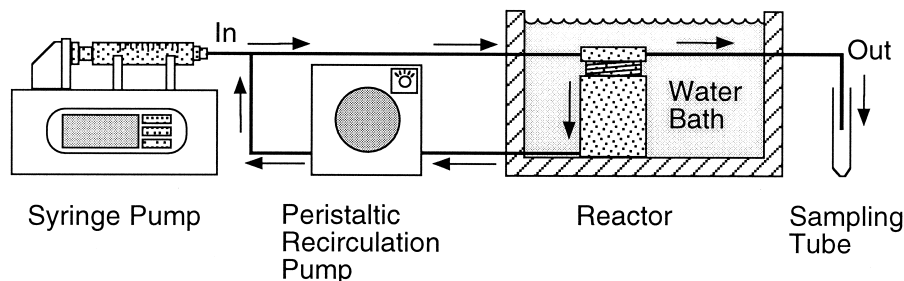


Fig. 1. Schematic diagram depicting the LTERR system employed in this study (after Weissbart, 1997).

QSI material under a binocular microscope revealed that the majority of the grains are elliptically shaped shards with prominent conchoidal fractures. In contrast, the Corning material fractured into more equant fragments; sharp, thin edges are uncommon. Surface areas in the starting materials were measured by using Brunauer-Emmett-Teller adsorption isotherm (BET) methods with Kr as the adsorbate and are reported in Tables 3, 4, and 5. Each new dissolution experiment began with a new lot of the pretreated material.

2.3. Experimental Design

We utilized three types of reactor systems to determine dissolution rates of $\text{SiO}_2(\text{am})$: (1) low temperature [40–80°C] externally recirculating flow through reactors (LTERR); (2) low temperature [60–80°C] batch reactors; and (3) hydrothermal [80–250°C] mixed flow reactors (HMFR). A schematic diagram of the LTERR is shown in Figure 1. This reactor design (Weissbart, 1997) was based upon the mixed flow methods introduced by Rimstidt and Dove (1986) for studies of mineral–water reaction rates. Reactor vessels were fashioned from solid rods of clear acrylic or laminated polycarbonate. The two main pieces of the reactor threaded together to form a cylinder 1.75 inches in diameter and ~3.75 inches high. The sample chamber consisted of a ring (either acrylic or polycarbonate) that is seated inside the reactor between the top and bottom pieces. At the bottom and top of the sample holder were a gasket and a piece of nylon mesh that prevented the sample from moving. The relatively large diameter of the sample holder (1.25-inch outer diameter, 1-inch inner diameter) allowed the silica samples to form a thin disk-like layer through which the solution flowed. This minimized flow dispersion and other hydrodynamic artifacts.

The LTERR experiments were conducted by injecting solutions into the system at rates of 2–12 $\mu\text{L}/\text{min}$ from glass syringes mounted on a Harvard PHD-2000 syringe pump (Harvard Apparatus, Holliston, MA, USA). The reactors were immersed in a 22-L constant temperature water bath and solution temperatures inside the reactors were measured by using *in situ* thermocouples. A peristaltic pump outside of the water bath rapidly recirculated the solution at rates of ~2.5 to 3.0 mL/min. The volume of the entire reactor–pump–tubing system was ~25 mL. A reaction time of ~7 to 21 days (seven residence times) was allowed to achieve steady-state conditions (e.g., discussion in Dove and Crerar, 1990).

The batch-reactor system consisted of polypropylene sample vials that each contained 0.5 or 1.0 g of silica glass and 20 or 25 mL of solution. The vials were submerged in a water bath and 1-mL solution samples were collected every 2 to 4 h to determine “initial rates” of reactions, with sampling times thereafter on the order of 8 to 12 h. Because of the possibility that apparent “initial rates” reflected dissolution of high-energy sites in the glass, these experiments were repeated using the same starting material until reproducible rates were achieved (typically 4 to 5 iterations).

The kinetics of $\text{SiO}_2(\text{am})$ dissolution at higher temperatures were measured in two HMFRs constructed of commercially pure titanium (e.g., Dove and Crerar, 1990). For each set of experiments, 2 to 4 g of the pretreated amorphous silica material were loaded into sample chambers of the reactors. Following a two day pretreatment period with deionized water (DIW) at 200°C, feed solutions were continuously pumped into the reactor vessel at a rate that held aqueous silica

concentrations far from equilibrium with respect to $\text{SiO}_2(\text{am})$ saturation. Experiments ran for 8 to 12 reactor volumes of fluid to assure steady-state conditions (i.e., complete exchange to the new solution) before sample collection. Typical flow-through rates were 1.5 to 6.5 mL/min.

All measurements of silica concentration were determined by the molybdate blue colorimetric method of Strickland and Parsons (1972). Absorption intensities were measured at the 810-nm wavelength and concentrations were determined using standards of known Si concentrations that were freshly prepared for each analysis session. Concentrations of Na in output solutions were confirmed by inductively-coupled plasma atomic emission spectroscopy (ICP-AES) methods as appropriate.

2.4. Measurement of Dissolution Rates

The overall dissolution reaction is monitored by the production of silicic acid, $\text{H}_4\text{SiO}_4(\text{aq})$, which forms by the congruent dissolution of $\text{SiO}_2(\text{am})$ into water:



As discussed in Dove and Rimstidt (1994), there is ample reason to assume that the primary dissolved species in these experiments is monomeric silicic acid because the experiments were designed to hold silica concentrations to relatively low values. Polynuclear species, such as $\text{H}_6\text{Si}_2\text{O}_7(\text{aq})$ (Cary et al., 1982; Alvarez and Sparks, 1985; Applin, 1987), may form in solutions containing high concentrations of silica, but these conditions are not germane to our experimental conditions.

The dissolution rates tabulated in Table 3 and 4 were calculated from the expression:

$$r_{\text{H}_4\text{SiO}_4} = \frac{(m_{\text{H}_4\text{SiO}_4, \text{out}} - m_{\text{H}_4\text{SiO}_4, \text{in}})\nu}{AM_s} \quad (3)$$

where:

- $r_{\text{H}_4\text{SiO}_4}$ = the rate of appearance of product (H_4SiO_4) at outlet conditions per unit area of reactant ($\text{mol m}^{-2} \text{s}^{-1}$)
- $m_{\text{H}_4\text{SiO}_4, \text{out}}$ = molal concentration at output (mol kg^{-1})
- $m_{\text{H}_4\text{SiO}_4, \text{in}}$ = molal concentration at input (mol kg^{-1}) ($m_{\text{H}_4\text{SiO}_4, \text{in}} = 0$)
- ν = mass flow rate (kg s^{-1})
- A = total surface area per g of solid in reactor ($\text{m}^2 \text{g}^{-1}$)
- M_s = mass of solid in reactor (g).

The measured macroscopic rate is applied to a pseudo first-order equation that is written in terms of silicic acid production (see Dove and Crerar, 1990):

$$r_{\text{H}_4\text{SiO}_4} = k_+ (a_{\text{SiO}_2})(a_{\text{H}_2\text{O}})^2 \left(1 - \frac{Q}{K}\right) \quad (4)$$

where k_+ is the reaction constant and the ratio, Q/K , describes the degree of saturation with respect to amorphous silica. Because the experiments are conducted far from equilibrium, Q/K is near zero and the activities of the reactants are near one. Hence, $r_{\text{H}_4\text{SiO}_4} \approx k_+$ and the dissolution rate constant is given by the molal flow rate, surface area of the reacting mineral, and the measured concentration of silicic acid at

Table 4. Experimental conditions and measured rates of SiO₂(am) dissolution by using low temperature externally recycled reactors (LTERR). Experiments were conducted at an in situ pH of 5.7.

Sample	Temp (°C)	NaCl conc. (molal)	Log average		Log rate (mol/m ² s)	Notes
			Flow rate (kg s)	Silica (molal)		
Corning Glass						
*3-1	40	0	-7.48	-5.11	-11.36	1
*3-2	40	0	-7.48	-4.92	-11.17	1
*1-1	60	0	-6.88	-5.07	-10.75	1
*1-2	60	0	-6.88	-5.12	-10.84	1
*4-1	60	0.01	-6.88	-4.85	-10.47	1
*4-2	60	0.01	-6.88	-5.14	-10.79	1
*4-3	60	0.03	-6.88	-5.14	-10.79	1
*4-4	60	0.03	-6.88	-5.26	-10.86	1
*1-3	60	0.03	-6.88	-4.48	-10.20	1
*1-4	60	0.05	-6.88	-4.09	-9.77	1, 2
*4-5	60	0.05	-6.88	-4.19	-9.82	1, 2
*4-6	60	0.05	-6.88	-4.75	-10.38	1, 2
*1-5	60	0.07	-6.88	-4.77	-10.32	1
*1-6	60	0.1	-6.88	-4.05	-9.71	1
*2-3	80	0	-6.78	-4.40	-9.96	1
*2-4	80	0	-6.78	-4.59	-10.13	1
QSI Glass						
*2-1	60	0	-6.78	-5.09	-10.63	3
*2-6	60	0	-6.78	-5.01	-10.57	3
*3-2	60	0	-6.88	-5.12	-10.65	3
*4-2	60	0	-6.88	-5.34	-10.99	3
*4-3	60	0.01	-6.88	-4.90	-10.55	3
*4-4	60	0.01	-6.88	-5.06	-10.72	3
*3-3	60	0.025	-6.88	-4.98	-10.63	3
*2-2	60	0.05	-6.78	-4.98	-10.54	3
*2-5	60	0.05	-6.78	-4.73	-10.29	3
*3-4	60	0.05	-6.88	-4.76	-10.41	3
*4-5	60	0.05	-6.88	-4.94	-10.58	3
*4-6	60	0.05	-6.88	-4.85	-10.47	3
*3-5	60	0.075	-6.88	-5.06	-10.65	3
*3-6	60	0.1	-6.88	-4.83	-10.43	3

1) Surface area = 0.0294 m²/g; 2) Plotted but not used in activation energy analysis; 3) Surface area = 0.0261 m²/g.

the outlet. The experiments and their corresponding reaction rates are discussed below.

3. RESULTS

3.1. Experiments in DIW

Dissolution rates were measured in DIW over the full temperature range (40–250°C) investigated in this study using the LTERR (40–80°C), batch (60–80°C), and the HMFR (80–250°C) reactor systems. Inspection of the data in Tables 3, 4, and 5 shows that the dissolution rates of the QSI and Corning glasses are similar within the experimental uncertainty despite differences in the manufacturing methods and their trace element chemistries. These results suggest that compositional differences between the two glasses do not significantly impact dissolution rates.

The temperature dependence of dissolution rates in DIW for the Corning and QSI glasses is shown in Figure 2a,b, respectively. The subset of experiments conducted at 125°C to 250°C in the HMFR displays a linear relationship between rate and inverse temperature. By fitting the Arrhenius relationship

Table 5. Experimental conditions and measured dissolution rates of SiO₂(am) by using the batch reactor systems. All experiments were conducted at an insitu pH of 5.7.

Sample	Temp (°C)	NaCl (molal)	Log time (s)	Log average		Notes
				Silica (molal)	Rate (mol/m ² /s)	
Corning Glass						
*1-1.1	60	0	5.18	-5.30	-10.97	1
*1-1.2	60	0	5.18	-5.55	-10.92	1
*1-2.1	60	0	5.38	-5.11	-10.98	1
*1-3.1	60	0	5.38	-5.36	-10.93	1
*11-1.1	60	0	5.18	-5.55	10.97	1
*11-2.1	60	0	4.87	-5.83	-10.93	1
*1-2.2	60	0.05	4.86	-4.24	-9.60	1
*1-3.2	60	0.05	4.86	-4.54	-9.60	1
*12-1.1	60	0.05	5.18	-4.21	-9.63	1
*12-1.2	60	0.05	4.87	-4.40	-9.50	1
QSI Glass						
*1-4.1a	60	0	4.18	-6.55	-11.05	1
*1-4.1b	60	0	4.18	-6.71	-11.22	1
*1-4.1c	60	0	4.18	-6.69	-11.20	1
*1-5.1a	60	0	4.94	-5.86	-11.15	1
*1-5.1b	60	0	4.94	-5.89	-11.18	1
*1-5.1c	60	0	4.94	-5.81	-11.09	1
*1-4.2	60	0.001	4.18	-6.02	-10.52	1
*1-5.2	60	0.001	4.94	-5.41	-10.70	1
*1-4.3	60	0.005	4.18	-5.58	-10.09	1
*1-5.3	60	0.005	4.94	-5.25	-10.53	1
*1-4.4	60	0.01	4.18	-5.27	-9.78	1
*1-5.4	60	0.01	4.94	-4.71	-9.99	1
*1-4.5	60	0.03	4.18	-5.14	-9.64	1
*1-5.5	60	0.03	4.94	-4.51	-9.79	1
*1-4.6	60	0.05	4.18	-5.00	-9.51	1
*1-5.6	60	0.05	4.94	-4.41	-9.70	1
*1-4.7	60	0.1	4.18	-4.89	-9.40	1
*1-5.7	60	0.1	4.94	-4.35	-9.63	1
*1-4.8	60	0.15	4.18	-4.78	-9.29	1
*1-5.8	60	0.15	4.94	-4.25	-9.53	1
*1-6.1a	80	0	4.77	-6.90	-10.28	1
*1-6.1b	80	0	4.77	-7.10	-10.47	1
*1-6.1c	80	0	4.77	-7.04	-10.41	1
*1-6.2	80	0.001	3.95	-7.45	-10.01	1
*1-6.3	80	0.005	3.95	-6.54	-9.09	1
*1-6.5	80	0.03	3.95	-6.46	-9.01	1
*1-6.6	80	0.05	3.95	-6.32	-8.88	1
*1-6.7	80	0.1	3.95	-6.25	-8.81	1
*1-6.8	80	0.15	3.95	-6.19	-8.74	1

1) Surface area = 0.08 m²/g.

$$\log k_+ = \log A - \frac{E_{a,sp}}{2.303R} \left(\frac{1}{T} \right) \quad (5)$$

to the data, apparent experimental activation energy ($E_{a,sp}$) values are obtained. These are the same for the QSI and Corning glass (76.4 ± 6.6 and 81.9 ± 3.0 kJ/mol, respectively) within experimental uncertainty.

Measurements of dissolution rates in DIW by using the LTERR show a systematic offset of ~0.4 log units faster than the rate predicted by the regression fit to hydrothermal data collected from the HMFR. A smaller offset is found for rates measured by using the batch-reactor system. Interpretation of these data, with respect to the merits and efficacies of the batch and LTERR systems, are discussed in Section 4.1.

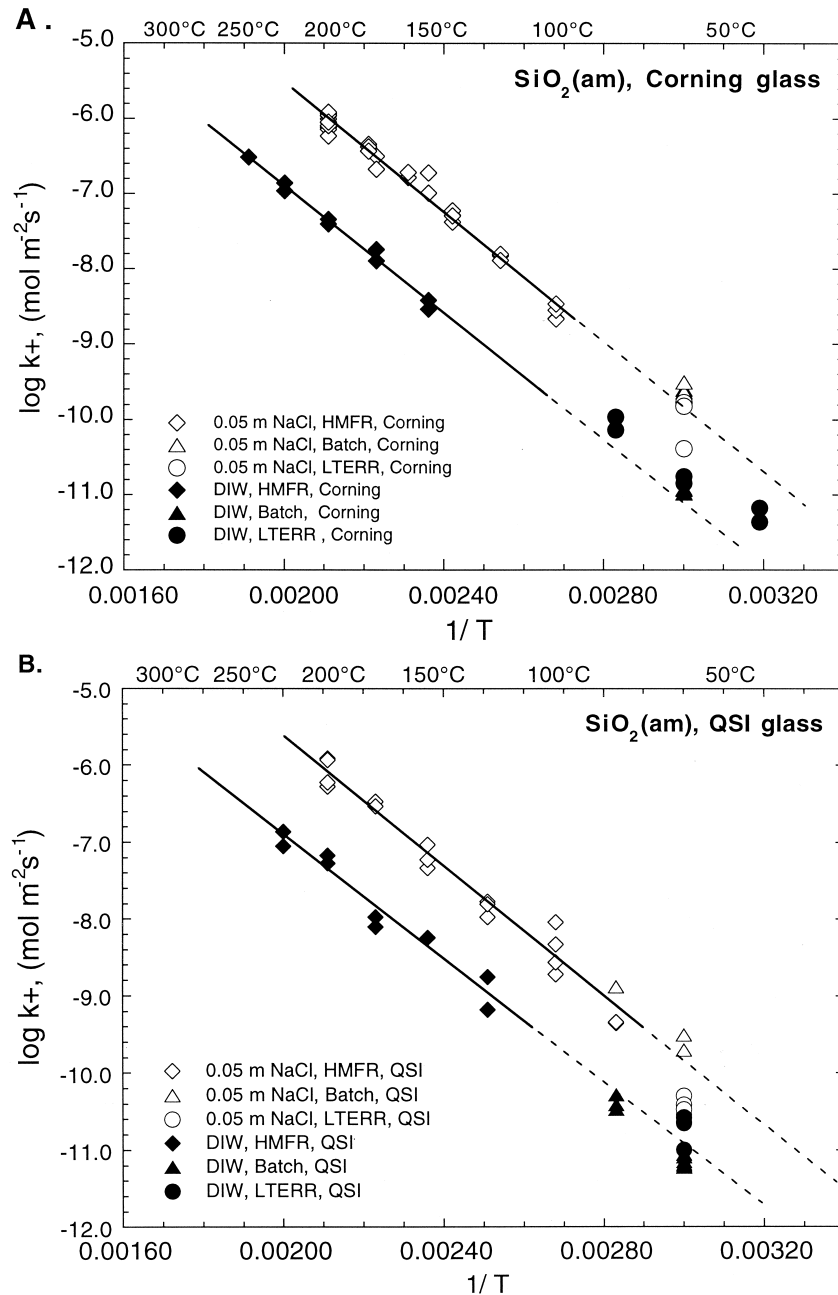


Fig. 2. Temperature dependence of amorphous silica dissolution kinetics in DIW and 0.05 molal NaCl solutions for: (A) Corning pyrolyzed silica and (B) QSI fused purified quartz. Arrhenius diagram illustrates that the addition of small amounts of NaCl does not change the activation energy of the reaction but enhances dissolution rates $\sim 21\times$ compared to rates measured in DIW. Calculated insitu pH is ~ 5.7 .

3.2. Experiments in NaCl Solutions

The kinetic data illustrated in Figure 3a,b,c show that dissolution rates of Corning (200°C) and QSI glass (60°C and 200°C) are enhanced by low concentrations of sodium in solution. Rates increase in response to increasing NaCl content over the low concentration (0 to 0.03 m) range. The data also show that dissolution rates increase by a factor of $\sim 21\times$ in 0.05 molal NaCl solutions compared to those measured in DIW

for both types of glass. Dissolution rates of amorphous silica remain roughly constant above 0.10 molal NaCl concentrations, which likely explains why Wirth and Geiskes (1979) did not observe differences in dissolution rates by varying solute concentrations. Their experiments were conducted at higher concentrations of sodium chloride (0.10–0.70 m) so, based on our results, we suggest that small changes in sodium concentration at high salinities do not have a pronounced effect on dissolution rates. Although the dissolution rates in DIW deter-

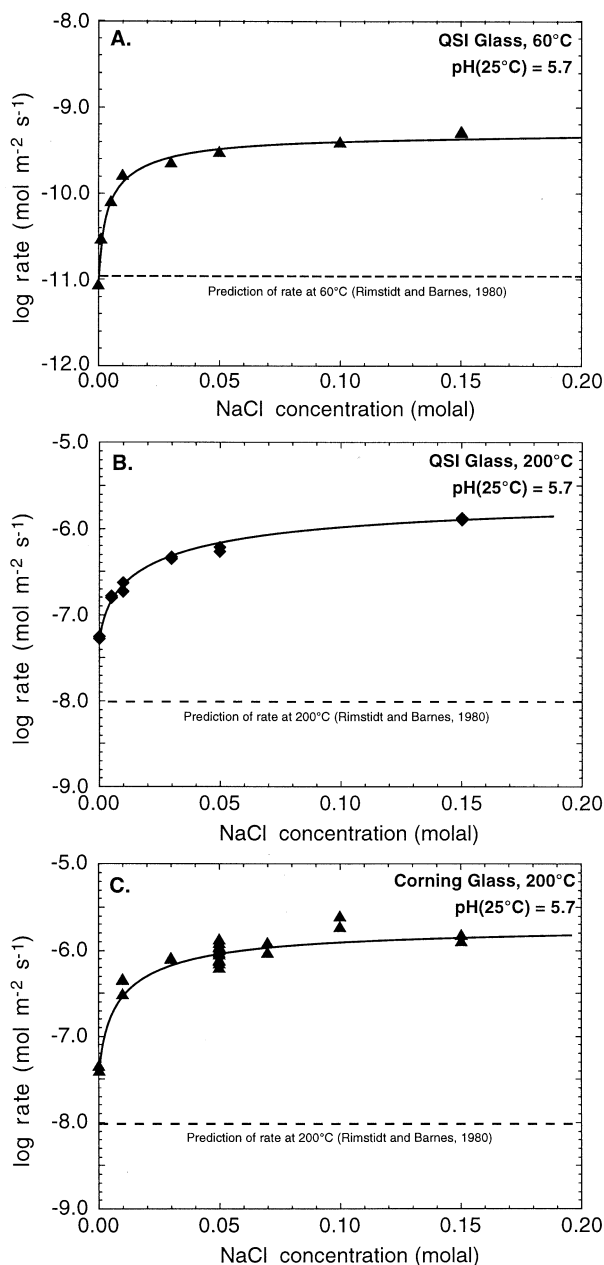


Fig. 3. Dissolution rates of amorphous silica exhibit sensitivity to sodium concentrations in solution. (A) QSI glass at 60°C; (B) QSI glass at 200°C; (C) Corning glass at 200°C. Rates increase with the introduction of low sodium contents and become approximately constant as NaCl concentrations exceed 0.10 molal. Note, too, that the experimentally determined rates in 0.10 molar NaCl are $\sim 100\times$ faster than the rates predicted (dashed line) by Rimstidt and Barnes (1980). Calculated insitu pH is ~ 5.7 .

mined in this study are in good agreement with the Rimstidt and Barnes (1980) calculations (e.g., Section 4.3), they predicted that electrolytes would cause small decreases in dissolution rates through reductions in the activity of water. Figure 3a,b,c show this is not the case.

The similarities in the magnitudes of rate enhancement at 200°C and 60°C seen in Figure 3a,b,c indicate that the temperature dependence of dissolution in 0.05 M NaCl solutions

should be approximately the same as those measured in DIW. This is confirmed by a linear regression of data collected by using the HMFR and shown in Figure 2a,b to obtain experimental activation energies of 83.4 ± 3.3 and 82.8 ± 1.9 kJ/mol for the QSI and Corning glasses, respectively. These values are similar to those obtained from the for DIW experiments (Table 6) within the uncertainties of the measurements.

4. DISCUSSION

4.1. Assessing Reactor Systems used in this Study

The data obtained by using the LTERR, HMFR, and batch-reactor systems yielded generally consistent results in DIW and NaCl solutions. However, rate measurements of Corning glass dissolution in DIW exhibited offset between the hydrothermal and low temperature measurements that we were unable to resolve (e.g., Fig. 2a). To evaluate this problem, we examined: 1) the effect of recirculation on in situ reactor temperatures; 2) the accuracy of flow-through rates; 3) the silica analysis to assure similar techniques across reactor methods; and also 4) measured the dissolution rate of quartz for the same systems. One potential problem was that LTERR vessels encountered repeated difficulties with short-term air locks at the inlet area. These locks repeatedly self-purged over the course of an individual experiment and the time-averaged behavior of the system did not appear to be significantly affected. After considerable analysis, we concluded that our particular configuration of the LTERR system yields reaction rates that are consistent with other kinetic methods only when net rates are faster than $\sim 10^{-12}$ mol m⁻² s⁻¹. This suggested that the slow dissolution reaction rates associated with amorphous silica in deionized water or quartz in any solution compositions could not be accurately measured by our LTERR systems due to possible experimental factors. Rates determined from batch reactors were consistent with the HMFR data within experimental errors and the absolute magnitude of the rate-enhancing effect ($\sim 21\times$) of sodium on the dissolution of amorphous silica was the same as measured by using the hydrothermal apparatus.

4.2. Estimates of Experimental Activation Energies

Few studies have reported estimates of experimental activation energies for the kinetics of amorphous silica dissolution. The summary in Table 6 shows that $E_{a,exp}$ values found in this study are generally higher than previous estimates except for the unusually large value reported by Mazer and Walther (1994) (93.7 ± 15.5 kJ/mol). As discussed earlier, the accuracy of their $E_{a,exp}$ may be impacted by the small size of the data set (three points) that spanned a relatively narrow temperature range of 40°C to 85°C. This confines confidence in the $E_{a,exp}$ values by magnifying the effect of possible experimental influences.

The values of $E_{a,exp}$ that we report for amorphous silica dissolution in deionized water fall within the range of values reported for α -quartz, as shown in Table 6. Taken collectively, the data suggest that SiO₂ (am) and quartz have the same $E_{a,exp}$. Furthermore, experiments by Renders et al. (1995) indicate that the activation energy of cristobalite dissolution is 68.9 ± 11 kJ/mol, which is within the experimental uncertainty of the quartz and amorphous silica data sets. If true, this implies that

Table 6. Summary of experimental activation energies reported for the dissolution kinetics of amorphous silica and quartz in 'pure' water and sodium-bearing solutions.

Reference	Type of silica or natural locale	Solution composition	Temp °C	$E_{a, xp}$ kJ/mol	Notes
<i>Amorphous silica</i>					
Rimstidt and Barnes (1980)	Fused quartz	Deionized water	25–300	60.9–64.9	
Mazer and Walther (1994)	Fused SiO ₂ powder	pH 4	40–85	93.7 ± 15.3	
This study (Corning glass)	SiO ₂ by pyrolysis	Deionized water	120–290	81.9 ± 3.0	
	SiO ₂ by pyrolysis	0.05 m NaCl	100–200	82.8 ± 1.9	
This study (QSI glass)	Fused quartz	Deionized water	140–290	76.4 ± 6.6	
	Fused quartz	0.05 m NaCl	80–200	83.4 ± 3.3	
This study	(compilation)	Deionized water	25–250	74.5 ± 1.4	1
<i>Quartz</i>					
Rimstidt and Barnes (1980)	Indiana aeolian sand	Deionized water	25–300	67.4–76.6	
Tester et al. (1994)	Brazilian	Deionized water	25–625	89 ± 5	
Polster (1994)	Arkansas, Ottawa	Deionized water	100–300	78.2 ± 2	
Gratz et al. (1990)	Brazilian	pH 10 to 13	148–236	86.41	2
	Brazilian	pH 10 to 13	148–236	90.22	3
House and Hickenbotham (1992)	Fontainbleau	pH 10	5–35	83.2	
Gratz and Bird (1993)	Brazilian	pH 10 to 13	148–236	78.6	
Dove (1994)	Arkansas	pH 2–12; Na = 0–0.3	25–300	66.03	4
Dove (1999)	Arkansas	Deionized water	175–290	72.0 ± 4	
	Arkansas	0.05 m NaCl	175–290	72.2 ± 6	

1) Regression does not include 18°C datum reported by Rimstidt and Barnes; 2) prism average; 3) rhomb average; 4) low-neutral pH range.

the rate-limiting step in the dissolution of silica polymorphs is the rupture of the Si-O bond, and reiterates the control of short-range forces on polymorph stability (e.g., Gibbs, 1982).

In the presence of sodium, the experimental activation energies for amorphous silica dissolution remain constant (Table 6). This is consistent with the results of earlier dissolution-rate studies of quartz (e.g., Dove and Crerar, 1990; Dove, 1994; Dove and Nix, 1997). The observation that rates are increased in these simple electrolyte solutions suggests that the introduction of cations increases the probability of crossing the reaction barrier without changing the reaction mechanism. This is an unusual circumstance as kinetic studies show that increases in reaction rates typically result from the lowering of energetic barriers between reactants and products (i.e., decrease $E_{a, xp}$). This type of behavior has implications for steric effects and that further suggests the indirect role of sodium in modifying the nucleophilic properties of water to result in enhanced reactivity. One means of rationalizing these findings is to consider that silica polymorphs carry a net negative surface charge when in aqueous solutions that have a pH exceeding ~3–4. Hence, dissolved cations in solution are attracted by electrostatic forces to the surface (e.g., Iler, 1979; Conway, 1981) such that solvated cations reside within the interfacial region. Disruption of the solvent network and the introduction of cations that impose their own solvation properties to the interfacial region contributes to an increase in the frequency of Si-O hydrolysis reactions. This promotes dissolution without a significant change in the energetics (c.f., Dove and Crerar, 1990; Dove, 1994; Dove and Nix, 1997). Eqn. 5 shows that changes in $\log k_+$ at a constant temperature occur when the experimental activation energy or the preexponential factor, A , vary. Values of $E_{a, xp}$ remain constant with the addition of sodium and the preexponential, which governs reaction frequency, increases. We predict that the dissolution rates of all silica polymorphs would exhibit similar dissolution behavior in NaCl solutions.

4.3. Evaluating all Reported Data to Determine the Temperature Dependence of Amorphous Silica Dissolution in 'Pure' Water

We compared the dissolution rates in DIW reported herein with rates published in the literature for measurements conducted in distilled, deionized or other forms of what we will call 'pure' water. In addition to determining a general temperature-dependent expression for dissolution rate constants, it was our hope that this analysis data would yield insight into the validity of our low temperature data that are arguably more uncertain than our higher temperature HMFR data (see Section 4.1). We plotted rate data from Rimstidt and Barnes (1980), Elmer and Nordberg (1958), Mazer and Walther (1994), and Seidel et al. (1997) along with our data for both types SiO₂(am) using the HMFR, LTERR, and batch systems. As is evident from Figure 4, the data reported by five different laboratories that used several different types of reactor systems agree remarkably well. The one datum that does not conform to this general rule is the 18°C rate reported by Rimstidt and Barnes (1980), which inexplicably plots at higher dissolution rates. When this point is excluded, a linear regression through the data set spanning 25°C to 250°C yields the Arrhenius expression (e.g., Eqn. 5):

$$\log k_+ = 0.82191 - 3892.3/T(K) \quad (6)$$

which is illustrated by the solid line in Figure 4. This gives an apparent activation energy for dissolution of 74.5 ± 1.4 kJ/mol. The $E_{a, xp}$ value is generally lower but similar within experimental uncertainty to the results reported in this study (see Table 6) and speaks to the validity of the data set over the large temperature interval and the various experimental apparatuses employed. Note that the method of SiO₂(am) synthesis apparently has no effect on the dissolution rate. The materials tested include fused quartz (this study and Rimstidt and Barnes,

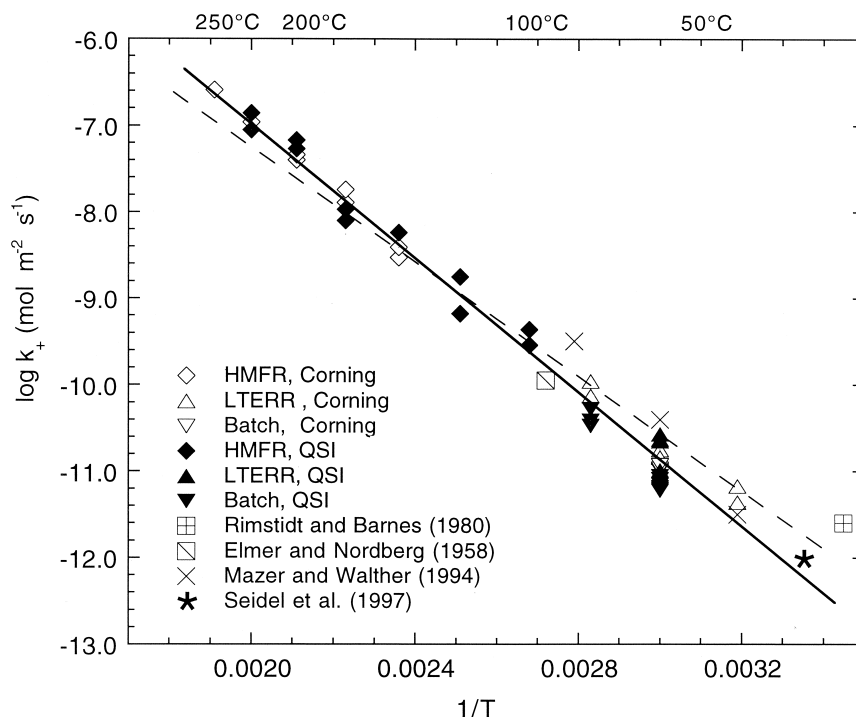


Fig. 4. Compilation of all published amorphous silica dissolution rates measured in solute-free water are plotted on an Arrhenius diagram. Diagram assumes that rate $\sim k_+$ (see Section 2.4). The solid line illustrates a regression fit through the entire data set, with the exception of one data point (see Section 4). For comparison, the dashed line shows the temperature dependence predicted by Rimstidt and Barnes (1980).

1980), fused SiO_2 powder (Mazer and Walther, 1994), SiO_2 by pyrolysis (this study), commercial amorphous silica (Seidel et al., 1997), and “porous leached glass” (Elmer and Nordberg, 1958). The predicted relationship between $\text{SiO}_2(\text{am})$ dissolution rate and temperature that Rimstidt and Barnes (1980) proposed is similar (dashed line, Fig. 4) to the regressed line described above. The similarity between the two lines is remarkable when one considers the scarcity of data on which the Rimstidt and Barnes (1980) prediction is based.

4.4. Comparison of SiO_2 Polymorphs Dissolution Rates

Recent theoretical models predict that the interactions of cations, such as sodium, with silica surfaces are weak for amorphous silica compared to quartz. The new rate data for $\text{SiO}_2(\text{am})$ present an opportunity to test this hypothesis by comparing physical and structural controls on the behavior of quartz and amorphous silica while holding chemical composition invariant. By evaluating the classical James and Healy (1972) equilibrium model of cation–surface interactions, Sverjensky (1993) and Sahai and Sverjensky (1997) presented a model that predicts the free energy of cation sorption, $\Delta G_{\text{ads}, \text{M}^{n+}}^\circ$, is modified by contributions from coulombic and solvation terms. Values of these terms depend upon the physical and chemical properties of the solid and solution (e.g., James and Healy, 1972). In practical terms, their model predicts that differences in the dielectric constant of the solids correlate with the cation–surface interaction strength, $K_{\text{S}, \text{M}^{n+}}$. Using the Sahai and Sverjensky (1997) notation, the relationship between $\log K_{\text{S}, \text{M}^{n+}}$ and $\Delta G_{\text{ads}, \text{M}^{n+}}^\circ$ is given by:

$$\log K_{\text{S}, \text{M}^{n+}} = \frac{\Delta G_{\text{ads}, \text{M}^{n+}}^\circ}{2.303RT} \quad (7)$$

where $\log K_{\text{S}, \text{M}^{n+}}$ describes equilibrium sorption of a 1:1 electrolyte at the β plane of the interface by a reaction with the general form:



The species, $>\text{SO}^-$, represents a negatively charged surface group. The cation–surface interaction strength is given by their model equation:

$$\log K_{\text{ads}, \text{M}^{n+}} = \frac{-\Delta\Omega_{\text{M}^{n+}}}{2.303RT} \left(\frac{1}{\epsilon_{\text{solid}}} \right) + \log K_{\text{ii}, \text{M}^{n+}}'' \quad (9)$$

where

$\Delta\Omega_{\text{M}^{n+}}$ = interfacial Born solvation coefficient for each cation

ϵ_{solid} = dielectric constant of the solid

$\log K_{\text{ii}, \text{M}^{n+}}''$ = non-intrinsic contribution to the free energy of adsorption

R = ideal gas constant ($8.3144 \times 10^{-3} \text{ kJ mol}^{-1} \text{ K}^{-1}$)

T = absolute temperature (K).

We use this model to calculate values of $\log K_{\text{S}, \text{M}^{n+}}$ for amorphous silica and quartz by substituting values for $\epsilon_{\text{SiO}_2(\text{am})}$ and ϵ_{quartz} (3.807 and 4.579, respectively, from Shannon, 1993) and the estimates of the $\Delta\Omega_{\text{M}^{n+}}$ and $\log K_{\text{ii}, \text{M}^{n+}}''$ from Sahai and Sverjensky (1997). The model predicts that $K_{\text{S}, \text{Na}^+}^{\text{SiO}_2(\text{am})}$ and

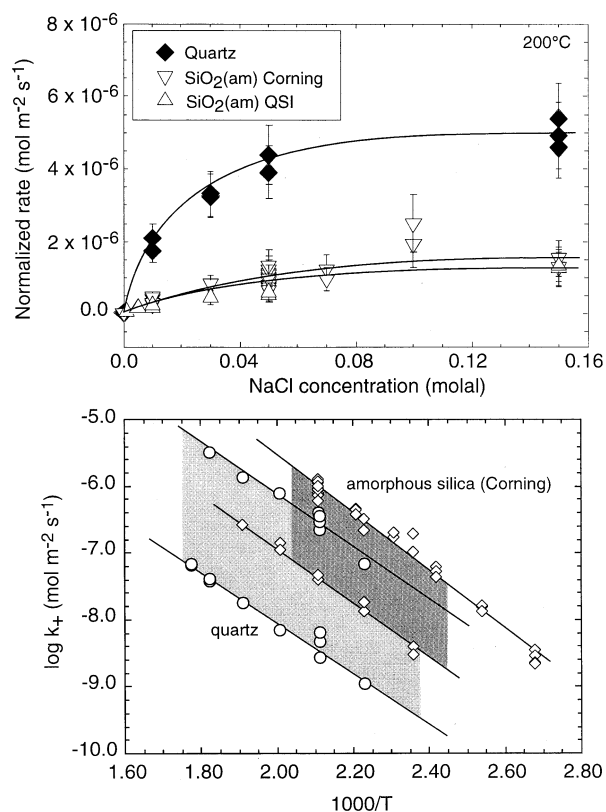


Fig. 5. Comparison of measured amorphous silica (Corning and QSI) and quartz dissolution rates by using data reported in this study and Dove (1999), respectively. (A) The dependence of quartz (◆) and amorphous silica (△) dissolution rates on sodium concentration at 200°C. Quartz dissolution rate data are normalized to amorphous silica rates to allow direct comparison of the rate-enhancing effect of NaCl. Data suggest a stronger dependence of quartz dissolution rates with increasing sodium concentration compared to amorphous silica. Error bars are 2σ uncertainties. (B) A similar, but offset, temperature dependence is exhibited for the range of experiments conducted in this study. Open circles denote quartz dissolution rates measured in DIW (lower trend) and 0.05 molal NaCl (higher trend). Open diamonds indicate amorphous silica dissolution rates in same solutions. Shaded areas illustrate the change in dissolution rate with the addition of sodium.

K_{S,Na^+}^{quartz} are equal to 10 and 23, respectively. That is, the interaction of sodium with the quartz surface is twice as strong for quartz as compared to $SiO_2(am)$. Figure 5a shows that these theoretical estimates appear to be consistent with experimental measurements. The amorphous silica (Corning) exhibits a weaker dependence upon increases in NaCl concentration than quartz. The difference in the rate-enhancing effect is $\sim 3\times$ under identical experimental conditions.

A weaker interaction of sodium with amorphous silica than with quartz is also upheld by fitting the rate vs. concentration data to an empirical Langmuir-type expression:

$$\text{rate} = k_{mx,Na^+} \left(\frac{K_{ads,Na^+}[m_{Na^+}]}{1 + K_{ads,Na^+}[m_{Na^+}]} \right) \quad (10)$$

where k_{mx,Na^+} is the maximum dissolution rate in NaCl solutions and $[m_{Na^+}]$ is the molal concentration of sodium (Dove,

1999). Because solution pH is invariant in the data used to evaluate Eqn. 10, an additional term for protons is not considered in this simple analysis. Values of $K_{ads,Na^+}^{SiO_2(am)}$ and K_{ads,Na^+}^{quartz} obtained by fitting Eqn. 10 to the 200°C experimental data collected for amorphous silica and quartz are 22 and 60, respectively (e.g., solid lines in Fig. 3a,b,c and Fig. 5a). Again, the estimates of $K_{ads,Na^+}^{SiO_2(am)}$ are roughly one third of that for K_{ads,Na^+}^{quartz} . Although our rate measurements are unable to firmly conclude that the interaction of sodium with the $SiO_2(am)$ surface is energetically less favorable compared to quartz, the data suggest this may be possible.

5. CONCLUSION

The dissolution kinetics of amorphous silica is quantified across the temperature range of 25°C to 250°C by using three types of reactors. The LTERR, HMFR, and batch-reactor systems give rates that are in general agreement but there are some inconsistencies at lower temperatures. The data show that the dissolution rates are independent of manufacturing process for all solutions tested. The data reported herein for DIW are in good agreement with previously published rates in 'pure' water over the temperature range 18°C to 250°C. Given that the various investigators employed a wide variety of experimental apparatuses, different water sources, as well as different amorphous silica materials, the consistency of the data set is remarkable. The kinetic findings reported herein should, therefore, be applicable to all types of amorphous silica in dilute, near pH neutral waters up to 250°C.

Rates of dissolution are increased by a factor of $\sim 21\times$ when low concentrations (≤ 0.05 molal) of NaCl are introduced to solution. This indicates that a major solute in the fluids of earth environments significantly enhances amorphous silica reactivity in dissolution processes. Combining our findings that amorphous silica and quartz are similarly enhanced by the presence of sodium chloride, we predict that other major solutes in terrestrial waters—potassium, magnesium and calcium—will also enhance the surface reactivity of amorphous silica in dissolution. Comprehensive models of silica behavior in the complex solution chemistries of natural waters will require a full assessment of these effects.

Acknowledgments—This work was supported by funding from the Petrology and Geochemistry Division of the National Science Foundation (Grant EAR-9405362 and EAR-9903349) and the Department of Energy, Environmental Management Science Program (Grant DE-FG07-96ER14699).

We thank Meg Grantham and Troy Lorier for invaluable laboratory assistance. JI expresses his gratitude to Drs. C. Koretsky, and J. D. Rimstidt for discussions of portions of the work encompassed by this paper. We also thank Quartz Scientific, and Dr. Jim Dickinson, Corning, for providing samples of the silica glass used in this study and J. D. Rimstidt for supplying us with the low temperature reactors utilized in the experiments.

REFERENCES

- Alvarez R. and Sparks D. L. (1985) Polymerization of silicate anions in solution at low concentrations. *Nature* **318**, 649–651.
 Applin K. R. (1987) The diffusion of dissolved silica in dilute aqueous solutions. *Geochim. Cosmochim. Acta* **51**, 2147–2151.
 Bennett P. C., Melcer M. E., Siegel D. I., and Hassett J. P. (1988) The dissolution of quartz in dilute aqueous solutions of organic acids at 25°C. *Geochim. Cosmochim. Acta* **52**, 1521–1530.

- Brady P. V. and Walther J. V. (1990) Kinetics of quartz dissolution at low temperatures. *Chem. Geol.* **82**, 253–264.
- Brückner R. (1970) Properties and structure of vitreous silica. *J. Non-Cryst. Solids* **5**, 123–216.
- Cary L. W., de Jong B. H. W. S. and Dibble W. E. Jr. (1982) A ^{29}Si NMR study of silica species in dilute aqueous solutions. *Geochim. Cosmochim. Acta* **46**, 1317–1320.
- Conway B. E. (1981) *Ionic Hydration in Chemistry and Biophysics*. Elsevier Scientific.
- Casey W. H. and Bunker B. (1990) Leaching of mineral and glass surfaces. In *Mineral–Water Interface Geochemistry* (eds. Hochella M. F. Jr. and White A. F.), Vol. 23, pp. 397–426. Mineralogical Society of America.
- Dove P. M. (1994) The dissolution kinetics of quartz in sodium chloride solutions at 25° to 300°C. *Am. J. Sci.* **294**, 665–712.
- Dove P. M. (1999) The dissolution kinetics of quartz in aqueous mixed cation solutions. *Geochim. Cosmochim. Acta* **63**, 3715–3727.
- Dove P. M. and Crerar D. A. (1990) Kinetics of quartz dissolution in electrolyte solutions using a hydrothermal mixed flow reactor. *Geochim. Cosmochim. Acta* **54**, 955–969.
- Dove P. M. and Rimstidt J. D. (1994) Silica–water interactions. In *Silica: Physical Behavior, Geochemistry and Materials Applications* (eds. Heaney P. J., Prewitt C. T., and Gibbs G. V.), Vol. 29, pp. 259–308. MSA Rev. Mineral.
- Dove P. M. and Nix C. J. (1997) The influence of the alkaline earth cations, magnesium, calcium, and barium on the dissolution kinetics of quartz. *Geochim. Cosmochim. Acta* **61**, 3329–3340.
- Elmer T. M. and Nordberg M. E. (1958) Solubility of silicon in nitric acid. *J. Am. Ceram. Soc.* **41**, 517–520.
- Fournier R. O., Rosenbauer R. J., and Bischoff J. L. (1982) The solubility of quartz in aqueous sodium chloride solutions. *Geochim. Cosmochim. Acta* **47**, 579–586.
- Gibbs G. V. (1982) Molecules as models for bonding in silicates. *Am. Mineral.* **67**, 421–450.
- Grambow B. (1985) A general rate equation for nuclear waste glass corrosion. Scientific Basis for Nuclear Waste Management XII. *Mat. Res. Soc. Symp. Proc.* **44**, 15–27.
- Gratz A. J. and Bird P. (1993) Quartz dissolution: Negative crystal experiments and a rate law. *Geochim. Cosmochim. Acta* **57**, 965–976.
- Gratz A. J., Bird P., and Quiro G. B. (1990) Dissolution of quartz in aqueous basic solution, 106–236°C: Surface kinetics of “perfect” crystallographic faces. *Geochim. Cosmochim. Acta* **54**, 2911–2922.
- House W. A. and Hickinbotham L. A. (1992) Dissolution kinetics of silica between 5 and 35°C. *J. Chem. Soc. Faraday Trans.* **88**, 2021–2026.
- House W. A. and Orr D. R. (1992) Investigation of the pH dependence of the kinetics of quartz dissolution at 25°C. *J. Chem. Soc. Faraday Trans.* **88**, 233–241.
- Iler R. (1979) *The Chemistry of Silica*. John Wiley and Sons.
- James R. O. and Healy T. W. (1972) Adsorption of hydrolyzable metal ions at the oxide–water interface III. A thermodynamic model of adsorption. *J. Coll. Int. Sci.* **40**, 65–81.
- Knauss K. G. and Wolery T. J. (1988) The dissolution kinetics of quartz as a function of pH and time at 70°C. *Geochim. Cosmochim. Acta* **52**, 43–53.
- Mazer J. J. and Walther J. V. (1994) Dissolution kinetics of silica glass as a function of pH between 40 and 85°C. *J. Non-Cryst. Solids* **170**, 32–45.
- Polster W. (1994) Hydrothermal precipitation and dissolution of silica Part 1. Conditions in geothermal fields and sedimentary basins, Part 2. Experimental evaluation of kinetics. Ph.D. Dissertation, Penn State Univ.
- Renders P. J. N., Gammons C. H., and Barnes H. L. (1995) Precipitation and dissolution rate constants for cristobalite from 150 to 300°C. *Geochim. Cosmochim. Acta* **59**, 77–85.
- Richert P. and Bottinga Y. (1984) Glass transitions and thermodynamic properties of amorphous SiO_2 , $\text{NaAlSi}_n\text{O}_{2n+2}$ and KAlSi_3O_8 . *Geochim. Cosmochim. Acta* **48**, 453–470.
- Rimstidt J. D. and Barnes H. L. (1980) The kinetics of silica–water reactions. *Geochim. Cosmochim. Acta* **44**, 1683–1699.
- Rimstidt J. D. and Dove P. M. (1986) Mineral/solution reaction rates in a mixed flow reactor: Wollastonite hydrolysis. *Geochim. Cosmochim. Acta* **50**, 2509–2516.
- Sverjensky D. A. (1993) Physical surface–complexation models for sorption at the mineral–water interface. *Nature* **364**, 766–780.
- Sahai N. and Sverjensky D. A. (1997) Solvation and electrostatic model for specific electrolyte adsorption. *Geochim. Cosmochim. Acta* **61**, 2827–2848.
- Shannon R. D. (1993) Dielectric polarizabilities of ions in oxides and fluorides. *J. Appl. Phys.* **73**, 348–366.
- Seidel A., Lobbus M., Vogelsberger W., and Sonnefeld J. (1997) The kinetics of dissolution of silica ‘Monospher’ into water at different concentrations of background electrolyte. *Solid State Ionics* **101–103**, 713–719.
- Strickland J. D. H. and Parsons T. R. (1972) Determination of reactive silica. In *A Practical Handbook of Seawater Analysis*. Fisheries Research Board of Canada.
- Tester J. W., Worley W. G., Robinson B. A., Grigsby C. O., and Feerer J. L. (1994) Correlating quartz dissolution kinetics in pure water from 25 to 625°C. *Geochim. Cosmochim. Acta* **58**, 2407–2420.
- Weissbart E. J. (1997) The leached layer formed on wollastonite in an acid environment. M.S. Thesis, VA Polytech. Inst. State Univ.
- Wirth G. S. and Gieskes J. M. (1979) The initial kinetics of dissolution of vitreous silica in aqueous media. *J. Coll. Int. Sci.* **68**, 492–500.